

A FULLY-DISTRIBUTED HETEROSTRUCTURE-BARRIER-VARACTOR NONLINEAR-TRANSMISSION-LINE FREQUENCY TRIPLER

Ming Li and R.G. Harrison

Department of Electronics, Carleton University, Ottawa, Canada K1S 5B6

Abstract—The discrete symmetric heterostructure - barrier varactor (HBV) was previously developed as an unbiased frequency-tripling device that needed no second-harmonic idler circuit. Other work investigated nonlinear transmission lines (NLTLs) using discrete varactors attached to linear guiding structures. Fully-distributed Schottky-varactor NLTLs were excessively lossy. This paper explores NLTLs based on *fully-distributed HBV structures*. Using both a modified FDTD method and numerical integration, it is shown that such NLTLs can provide efficient tripling over a wider range of input bandwidth than is possible with fixed-tuned triplers.

I. INTRODUCTION

Heterostructure-barrier varactors(HBV) with symmetrical $C(v)$ and antisymmetrical $i(v)$ characteristics[1]-[7] have thin large-bandgap barriers sandwiched between thick smaller-bandgap layers. The even $C(v)$ symmetry yields high-power frequency multipliers [4], [8] whose output spectra contain only odd-order harmonics. Maximum nonlinearity occurs at $v = 0$ V, obviating bias circuits.

Efficient multipliers need HBVs with large C_{max}/C_{min} ratios and small leakage currents. Due to excessive leakage, earlier HBVs fabricated on GaAs [1][2] and InP [3] had low Q. The resulting triplers had efficiencies < 5% and low outputs $P_{out} \sim 2$ mW. P_{out} -saturation occurred at low P_{in} levels. These shortcomings can be avoided by using the *stacked* HBV structure of [4]. The InGaAs /InAlAs system provides both effective current blocking and low-resistance contacts [5].

With n stacked varactors, P_{out} -capability increases as n^2 , while the capacitance decreases as n [5][6]. A tuned (non-distributed) 3-stack HBV tripler had a measured 20% efficiency for $P_{out} = 100$ mW at 39 GHz [4].

Other work [7] investigated NLTLs made by periodically loading conventional lines with discrete varactors. NLTLs using *distributed* Schottky varactor structures were too lossy [7].

Here we investigate fully-distributed NLTLs using the

improved HBV structure. From an incremental NLTL equivalent circuit we derive a nonlinear wave equation. This is solved numerically by the FDTD method, using appropriate initial and boundary conditions. As a check, the NLTL is also modeled directly using Libra [13]; time domain integration yields the transient solution. The waveform and spectra obtained by the two methods agree excellently. Simulations show these NLTLs can provide efficient tripling over a wider frequency range than provided by fixed-tuned triplers.

II. DEVICE MODEL AND WAVE EQUATION

The structure of the fully-distributed NLTL is shown in Fig. 1.

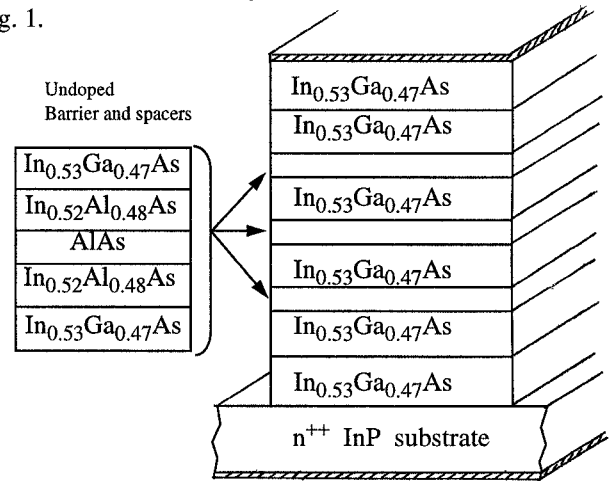


Fig. 1 Cross-section of stacked HBV structure. The MBE layers are similar to those in [5].

The idea is to extend the HBV device in a “horizontal” direction to form an NLTL. At the high frequencies for which it is well suited, such a NLTL would be of the order of ~ 100 μm long and 10 μm wide. Fig. 2 shows the equivalent circuit of an infinitesimal section of the NLTL. Here $i(z, t)$ is the current entering a section of length dz at location z and instant t , while $v(z, t)$ is the corresponding voltage between the top and bottom metal contacts. L_z is the inductance/length, and $q_z(v)$ is the charge/ length.

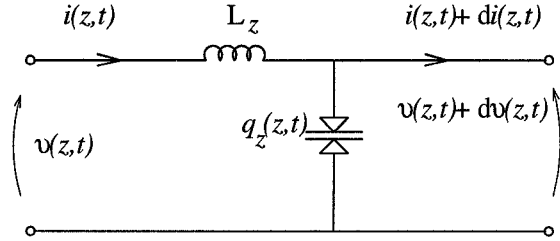


Fig. 2 Equivalent circuit of length dz of distributed NLTL.

Following [9], we assume the empirical $v(q_z)$ relation

$$\alpha v(z, t) = \frac{q_z(z, t)}{q_{z0}} + \beta \left(\frac{q_z(z, t)}{q_{z0}} \right)^3 \quad (1)$$

where α , β and q_{z0} characterize HBV. From (1) and Fig. 2 we obtain the nonlinear wave equation

$$\frac{\partial^2}{\partial z^2} [x + \beta x^3] = \frac{1}{u^2} \frac{\partial^2 x}{\partial t^2} \quad (2)$$

where $x(z, t) = q_z(z, t)/q_{z0}$ is the normalized charge/length, $u = 1/(\sqrt{C_{z0} \cdot L_z})$ is a velocity, and $C_{z0} = \alpha q_{z0}$ is the capacitance/length at zero bias.

III. THE NLTL SIMULATION

We simulate the NLTL (a) using a modified FDTD method and (b) by numerical integration.

(a) The FDTD method was previously combined with TLM for time-domain simulations of nonlinear devices [10] or transmission lines [11]; the advantages being that the TLM models physical wave propagation, while FDTD offers computational efficiency. Our algorithm resembles [10], except that instead of Maxwell's curl equations, we use the nonlinear wave equation (2) to describe wave propagation. Whereas general FDTD or TLM methods require 6 (field) variables, our algorithm needs only one: the normalized charge x , and is consequently much less computer-intensive. Furthermore, by using an empirical q - v relationship such as (1), it is easy to augment the equivalent circuit for improved accuracy.

Applying FDTD [12] to the wave equation (2), we obtain

$$\begin{aligned} x_{i,n+1} &= 2 \cdot x_{i,n} - x_{i,n-1} \\ &+ k^2 \cdot \mu^2 \cdot \left[\frac{x_{i-1,n} - 2 \cdot x_{i,n} + x_{i+1,n}}{h^2} \cdot (1 + 3 \cdot \beta \cdot x_{i,n}^2) \right] \\ &+ \frac{3 \cdot k^2 \cdot \mu^2 \cdot \beta \cdot x_{i,n}}{2 \cdot h^2} (x_{i+1,n} - x_{i-1,n})^2. \end{aligned} \quad (3)$$

In (3), the normalized charge $x(z, t)$ is discretized in

space and time as

$$x_{i,n} = x(ih, nk)$$

where $h = \Delta z$ and $k = \Delta t$ are space and time increments, and i and n are integers.

Fig. 3 shows a complete equivalent circuit of the NLTL.

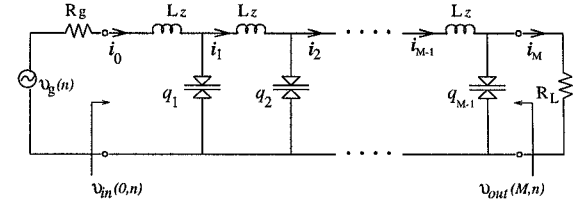


Fig. 3 A complete equivalent circuit of the NLTL.

The boundary conditions are

$$v_{in}(0, n) = v_g(n) - i_0 \cdot R_g \quad (4)$$

$$v_{out}(M, n) = i_M \cdot R_L \quad (5)$$

where R_g and R_L are generator and load resistances, and the equivalent circuit consists of M subsections. The physical length of the NLTL is $l = Mh$.

Application of Kirchhoff's current law and FDTD [12] to Fig. 3 results in

$$i_0 = i_1 + q_{z0} \cdot h \cdot \frac{x_{1,n} - x_{1,n-2}}{2 \cdot k}$$

$$i_1 = i_2 + q_{z0} \cdot h \cdot \frac{x_{2,n-1} - x_{2,n-3}}{2 \cdot k}$$

:

:

$$i_M = i_{M-1} - q_{z0} \cdot h \cdot \frac{x_{M-1,n} - x_{M-1,n-2}}{2 \cdot k}$$

$$i_{M-1} = i_{M-2} - q_{z0} \cdot h \cdot \frac{x_{M-2,n-1} - x_{M-2,n-3}}{2 \cdot k}$$

:

:

Combining (4) and (5) with (1), the boundary and initial conditions can be satisfied.

(b) The numerical integration approach involves simulating the NLTL in Libra 6.0 [13]. The procedure is:

(i) Use curve fitting to represent the $C(v)$ relation of (1) by the polynomial

$$C(v) = c_0 + c_1 \cdot v + c_2 \cdot v^2 + \dots + c_m \cdot v^m \quad (6)$$

Here $C(v) = d q_z / d v$ and the coefficients, $c_0, c_1, c_2, \dots, c_m$, depend on the constants, α, β and q_{z0} . The number of the coefficients used here was $m \sim 20$.

(ii) Use (6) as the nonlinear capacitor model in Libra, and build the equivalent circuit of the NLTL.

(iii) Do time-domain simulations using the "Transient

Bench" numerical integration procedure of Libra. Fig. 4 compares the NLTL output voltage waveforms as predicted by the two methods when the input is a 30-GHz 1.0-V sinewave. For the FDTD simulation, the equivalent circuit of Fig. 3 used $M = 25$ subsections. Each subsection corresponds to a discrete HBV of area $27 \times 27(\mu\text{m})^2$, for an NLTL of width 27 μm , and total length of $25 \times 27\mu\text{m} = 0.67\text{mm}$. The parameters of each section are $\alpha=1.0$, $\beta=3.0$, $L_zh=0.05\text{ nH}$, $C_zh=0.1\text{ pF}$, $R_sh=1.0\Omega$ (shunt resistance). Fig. 4 shows good agreement between the FDTD and numerical-integration methods.

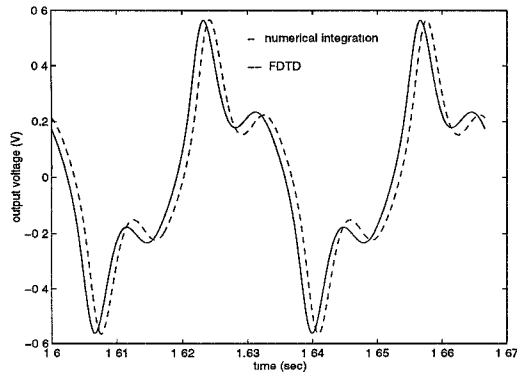


Fig. 4 NLTL time-domain simulation.

IV. RESULTS AND DISCUSSION

Modes of Operation: To investigate the NLTL behavior as a distributed frequency multiplier for different input frequencies f_{in} , we assumed an NLTL of length = 1.35 mm ($M = 50$ subsections), with the parameters per-subsection of $\alpha=1.0$, $\beta=3.0$, $L_zh=0.05\text{ nH}$, $C_zh=0.1\text{ pF}$, $R_sh=0.5\Omega$. Fig. 5 shows the simulated output waveform when $f_{in}=29\text{ GHz}$.

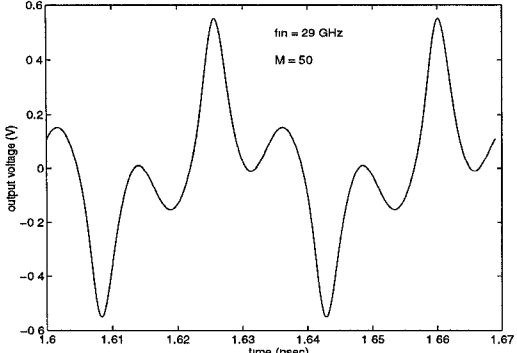


Fig. 5(a) NLTL time-domain response for $l=1.35\text{ mm}$, $f_{in}=29\text{ GHz}$, and $P_{in}=4\text{ dBm}$.

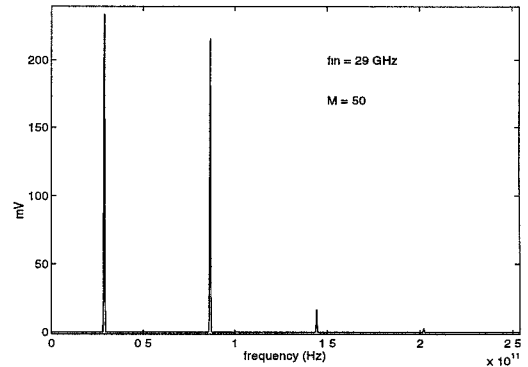


Fig. 5(b) NLTL spectrum for $l=1.35\text{mm}$ ($M=50$), $f_{in}=29\text{ GHz}$, and $P_{in}=4\text{ dBm}$.

Fig. 5(b) is the corresponding spectrum, showing good tripler operation with $f_{out}=87\text{ GHz}$, a 3rd-harmonic / fundamental power ratio of -0.28 dB, and conversion loss of 5.1 dB. All even harmonics are suppressed by the $C(v)$ symmetry, enhancing the conversion efficiency.

Fig. 6(a) depicts the waveform when f_{in} is reduced to 20 GHz : higher-harmonic content is now evident.

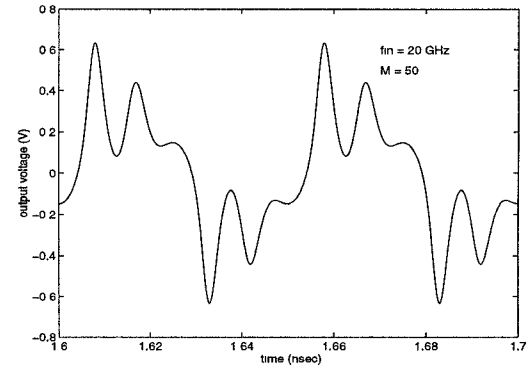


Fig. 6(a) NLTL output waveform for $l=1.35\text{mm}$, $f_{in}=20\text{ GHz}$, and $P_{in}=4\text{ dBm}$.

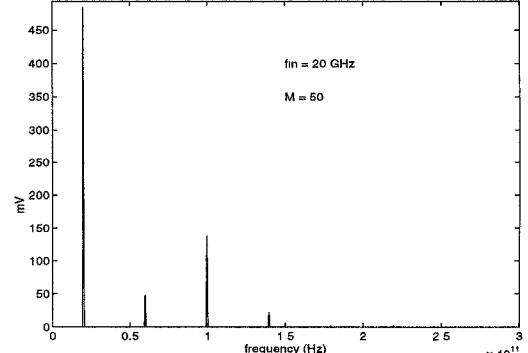


Fig. 6(b) NLTL spectrum for $l=1.35\text{mm}$, $f_{in}=20\text{ GHz}$, and $P_{in}=4\text{ dBm}$.

As seen in Fig. 6(b), the 5th harmonic is now larger than the 3rd, and the NLTL is operating as a quintupler.

Optimization: To optimize as a tripler, we:

- (i) Set $f_{in} = 30$ GHz and varied the NLTL length over the range $0.54\text{ mm} \leq l \leq 1.89\text{ mm}$ ($20 \leq M \leq 70$)
- (ii) Set $l = 1.35$ mm ($M = 50$) and varied the input frequency over the range $20 \leq f_{in} \leq 30$ GHz.

Fig. 7 shows that for experiment (i) the optimum length is 1.35 mm, yielding a power ratio of -1.69 dB. (compared with the -0.28 dB for $f_{in}=29$ GHz). The power ratio remains better than -3.0 dB over the range $1.08\text{ mm} \leq l \leq 1.62\text{ mm}$ ($40 \leq M \leq 60$).

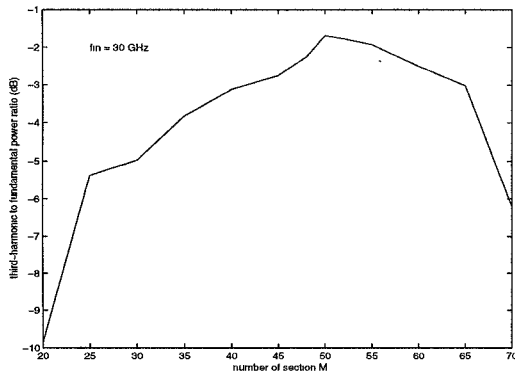


Fig. 7 3rd-harmonic to fundamental power ratio versus NLTL length l (M), when $f_{in}=30$ GHz.

For experiment (ii) Fig. 8 shows an effective input 3-dB bandwidth of 25 to 31.5 GHz, the corresponding output range being 75 to 94.5 GHz.

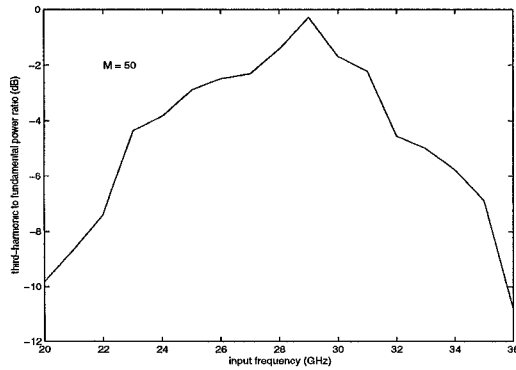


Fig. 8 3rd-harmonic to fundamental power ratio versus input frequency f_{in} , when $l=1.35$ mm ($M=50$).

V. CONCLUSION

A fully-distributed NLTL incorporating an extended HBV structure is reported. Nonlinear transient analysis is

carried out using both FDTD and numerical-integration methods. The results indicate that this new device is promising as an *untuned* wideband frequency multiplier, with potential in millimeter-wave communications. Further work will be directed to optimizing the parameters of the NLTL and its embedding for efficient harmonic generation for specified output powers levels and bandwidths.

ACKNOWLEDGEMENT

This work was supported by a grant from the Natural Sciences and Engineering Research Council of Canada.

References

- [1] A. Rydberg, H. Grönqvist and E.L. Kollberg, "Millimeter and submillimeter-wave multipliers using quantum barrier varactor (QBV) diodes," *IEEE Electron Device Lett.*, 11, (9), pp. 373-375, 1990
- [2] H.X. Liu, L.B. Sjøgren, C.W. Domier, N.C. Luhmann, D.L. Sivco and A.Y. Cho, "Monolithic quasi-optical frequency tripler array with 5 W output power at 99 GHz," *IEEE Electron Device Lett.*, 14, (7), pp. 329-331, 1993
- [3] T.J. Tolmunen, A.V. Räisänen, E. Brown, H. Grönqvist and S.M. Nilsen, "Experiments with single barrier varactor tripler and quintupler at millimeter wavelengths," *Proceedings of the International Symposium on Space Terahertz Technology*, 1994
- [4] K. Krishnamurthi and R.G. Harrison, "Millimeter-wave frequency tripling using stacked heterostructure-barrier varactors on InP," *IEE Proc. Microw. Antennas Propag.*, Vol. 143, 1996
- [5] K. Krishnamurthi, "Heterostructure Varactors on InP and GaAs for Millimeter-Wave Frequency Triplers," Ph.D. Dissertation, Carleton U., January 1995.
- [6] A. Rahal, E. Boch, C. Rogers, J. Ovey and R.G. Bosisio, "Planar multi-stack quantum barrier varactor tripler evaluation at W-band," *IEEE Electronics Letters*, Vol. 31, No. 23, 1995
- [7] H. Shi, W.M. Zhang, C.W. Domier, N.C. Luhmann, L.B. Sjøgren and H.X. Liu, "Novel concepts for improved nonlinear transmission line performance," *IEEE Trans. Microwave Theory Tech.*, Vol. 43, pp. 780-788, 1995
- [8] R.J. Baker, D.J. Hodder, B.P. Johnson, P.C. Subedi and D.C. Williams, "Generation of kilovolt-subnanosecond pulses using a nonlinear transmission line," *Measurement Science & Technology*, Vol. 4, No. 8, pp. 893-895, 1993
- [9] K. Krishnamurthi and R.G. Harrison, "Analysis of symmetric-varactor frequency triplers," *IEEE International Microwave Symposium Digest*, pp. 649-652, June 1993
- [10] R.H. Voelker and R.J. Lomax, "A Finite-difference transmission line matrix method incorporating a nonlinear device model," *IEEE Trans. Microwave Theory Tech.*, Vol. 38, No. 3, pp. 302-312, 1990.
- [11] J. Xu and J.M. Chuang, "Modeling of nonlinear-optical media with the TLM-based finite-difference-time-domain method," *Microwave and Optical Technology Letters*, Vol. 13, pp. 259-264, 1996
- [12] Robert L. Ketter, *Modern Methods of Engineering Computation*, New York: McGraw-Hill, 1969.
- [13] *Libra 6.0*, Hewlett-Packard Company, 1995